Production Systems and Information Engineering, Miskolc, Vol. 1. (2003), pp. 3-16

NUMERICAL SIMULATION FOR THE DETERMINATION OF THE TEMPERATURE FIELDS AND THE HEAT AFFECTED ZONES IN GRINDING

ATHANASIOS G. MAMALIS
Manufacturing Technology Division, National Technical University of Athens
GR 10682 ATHENS, Greece
mamalis@central.ntua.gr

JÁNOS KUNDRÁK
Department of Production Engineering, University of Miskolc
H-3515 MISKOLC, Hungary
kundrak@gold.uni-miskolc.hu

ANGELOS MARKOPOULOS
Manufacturing Technology Division, National Technical University of Athens
GR 10682 ATHENS, Greece
amark@central.ntua.gr

[Received October 2002 and accepted February 2003]

Abstract. A finite element model is proposed for the simulation of grinding of hardened steels with aluminium oxide wheels. For this task the implicit FEM code MARC is used. The proposed model is a transient state, non-linear problem that can calculate the maximum temperature and the temperature fields on the ground workpiece. The input data required for the analysis are provided through a series of grinding experiments. From the numerical results obtained from the analysis it is possible to predict the size of the heat affected zones of the workpiece.

Keywords: Surface grinding, Finite Element Method, Heat affected zones

1. Introduction

Grinding modelling has been a main concern of the researchers dealing with this process due to the difficulties raised in its experimental studying. A lot of models have been used for the mechanical and thermal simulation of grinding and of its components, mainly the workpiece, the grinding wheel, the chip and the coolant. Especially, the thermal modelling of grinding has been extensively investigated because of the importance of the knowledge of the maximum temperature reached during the process and, consequently, of the thermal damage induced to the workpiece because of excessive heat loading. This heat input is responsible for a number of defects in the workpiece like metallurgical alterations, microcracks and residual stresses. The areas of the workpiece that are affected are described as heat affected zones.

An overview of grinding models can be found in Refs [1, 2], where the former lists the majority of models developed for grinding while the latter focuses on thermal modelling.

Since the publications of these references some numerical models and especially Finite Element Method (FEM) models have enriched the relative literature [3-6]. The advances in computers and the introduction of user-friendly FEM software for PCs have given a new turn on the simulation of grinding.

Numerical two-dimensional (2D) and three-dimensional (3D) thermal models using the implicit Finite Element Method (FEM) code MARC in order to simulate grinding have already been presented by the authors [7, 8]. In the present paper the validation of the 2D model was considered when grinding bearing steel 100Cr6 with aluminium oxide wheels. The calculation of the maximum temperature, the distribution of temperature fields developed during grinding and the prediction of the heat affected zones in the workpiece are presented and discussed.

2. FEM modelling of grinding

Almost all models on the thermal modelling of grinding are based on the publication of Jaeger on moving heat sources [9]. In Jaeger's model the grinding wheel is represented by a heat source moving along the surface of the workpiece with a speed equal to the workspeed, see Fig. 1. A two dimensional model is used, provided that the grinding width is large with respect to its length. However, this model is based on the assumption that the total grinding energy is entirely absorbed by the workpiece, whilst in reality the total grinding energy is distributed in the workpiece, the grinding wheel, the chip and the coolant. The initial model was improved by studying the percentage of the total heat entering the workpiece and the effect of cutting fluid on the maximum temperature [10-13] and by the introduction of models where heat capacity and heat conductivity are temperature dependent [6].

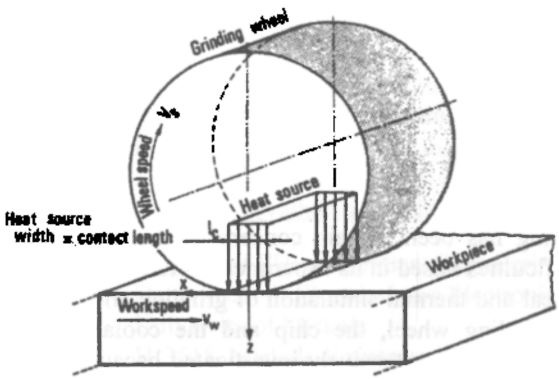

Fig. 1: Jaeger's model [2]

In the present paper a FEM model, based on Jaeger's model, is proposed for the simulation of the grinding process. The model configuration is presented in Fig. 2. On the top surface of the workpiece heat is entering the workpiece, in the form of heat flux, Q, input that moves along this surface. Cooling is simulated by means of convective boundary conditions. All the other sides of the workpiece are considered to be adiabatic, and so no heat exchange takes place in these sides. The model has a length of 35 mm and a height of 5 mm, sufficient enough for the temperature fields to be fully deployed and observed in full length. A mesh is applied on the proposed model, consisting of 1400 4-noded quadrilateral elements and 1491 nodes. The mesh is denser towards the grinding surface, that is the thermally loaded surface, and, thus the most affected zone of the workpiece, allowing for greater accuracy to be obtained.

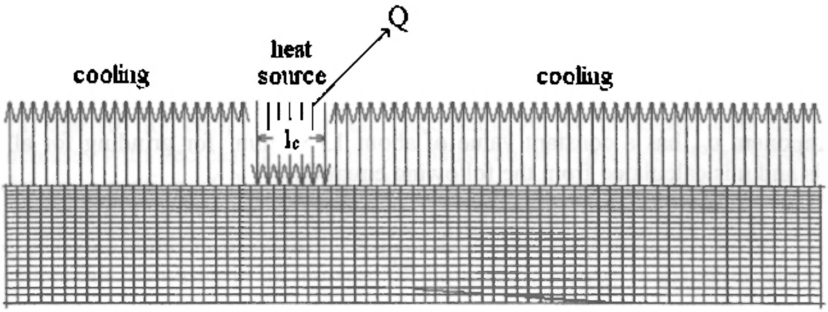

Fig. 2: Suggested thermal finite element model for surface grinding

As mentioned above, the heat source is characterized by a physical quantity, the heat flux, Q, that represents the heat entering the workpiece per unit time and area and it is considered to be of the same density along its length, taken equal to the geometrical contact length, l_c, which is calculated from the relation

$$l_c = \sqrt{a \cdot d_s} \tag{1}$$

where a is the depth of cut and d_s the diameter of the grinding wheel. The real contact length is expected to be bigger due to the deflection of the grinding wheel and the workpiece in the contact area. Nevertheless, the geometrical and real contact lengths are considered to be equal. The heat flux can be calculated from the following equation

$$Q = \varepsilon \frac{F_t' v_s}{l_c} \tag{2}$$

where ε is the percentage of heat flux entering the workpiece, F'_t the tangential force per unit width of the workpiece, v_s the peripheral wheel speed and l_c the geometrical contact length. The proportion of the heat flux entering the workpiece can be calculated by a formula suggested by Malkin for grinding with aluminium oxide wheels, by making assumptions on the partitioning of total specific grinding energy, u, required for grinding [14]. The total specific grinding energy consists of three different components: the specific energy required for the formation and the removal of the chip, u_{ch}, the specific energy required for plowing, i.e. the plastic deformation in the regions where the grains penetrate the workpiece surface but no material is removed, u_{pl} and the specific energy required for making the flat wear grains slide on the workpiece surface, u_{sl}, thus

$$u = u_{ch} + u_{pl} + u_{sl} \tag{3}$$

It has been analytically and experimentally shown that approximately 55% of the chip formation energy and all the plowing and sliding energy are conducted as heat into the workpiece, i.e.

$$\varepsilon = \frac{0.55 \cdot u_{ch} + u_{pl} + u_{sl}}{u} = \frac{u - 0.45 \cdot u_{ch}}{u} \Rightarrow \varepsilon = 1 - 0.45 \frac{u_{ch}}{u} \tag{4}$$

The component u_{ch} has a constant value of about 13.8 J/mm^3 for grinding for all ferrous materials and u is calculated from the following equation:

$$u = \frac{F_t' v_s}{a v_w} \tag{5}$$

where v_w is the workspeed and, consequently, as in Jaeger's model, the speed of the moving heat source. Note that, in both equations (2) and (5) the value of F'_t is needed in order to calculate the heat flux and the total specific grinding energy, respectively; it can be calculated from

$$F_t' = \frac{P_t'}{v_s} \tag{6}$$

where P'_t is the power per unit width of the workpiece, which was measured during the testing of the different grinding wheels, as described in the next paragraph. The kind of modelling suggested in this paper is suitable for grinding process with very small depth of cut, since there is no modelling of the chip.

Note that, in thermal modelling there are two kinds of problems that are being dealt with: the steady-state and the transient problems. In the former it is assumed that the temperature is constant in respect with time, i.e. $\dot{T} = \partial T/\partial t = 0$, while in the latter $\dot{T} \neq 0$, as is the case in the presented model. Furthermore, the two coefficients of the workpiece material that are related to temperature, i.e. the thermal conductivity and the specific heat capacity, along with the density of the workpiece need to be inserted as input to the program. Especially the first two were considered to be temperature depended and they were taken from the FEM program material properties data bank. Transient conditions and temperature depended material properties produce non-linear finite element problems, which are more difficult to be solved. The algorithm and the formulae used for the solution of such problems by MARC, which is an implicit FEM software, are given in Appendix 1.

3. Experimental results

Six aluminium oxide grinding wheels of the same diameter, d_s=250 mm and width b_s=20 mm with different bonding were used on a BRH 20 surface grinder. Two depths of cut were used, namely 0.02 mm and 0.05 mm while the workpiece speed was v_w=8 m/min and the wheel speed v_s=28 m/s kept constant for both sets of experiments, for all wheels. The workpiece material was the 100Cr6 bearing steel. Throughout the process the synthetic coolant Syntilo-4 was applied at 15 ℓ/min. For each grinding wheel, 10 passes of the same depth of cut were performed over the workpiece. The power per unit width of the workpiece was measured for each pass and its average value was calculated. For measuring the power, a precision three-phase wattmeter was used. First, the power of the idle grinding machine was measured and set as the zero point of the instrument. Then, the workpieces were properly ground and the power was registered on the measuring device. After 10 passes were performed the grinding wheel was dressed with a single point diamond dressing tool, with depth a_d=0.02 mm and feed of f_d=0.1-0.2 mm/wheel rev. The measured quantities, as well as the quantities calculated from equations (1)-(6), are tabulated in Table 1 (a) and (b) for each depth of cut. According to the measured data the specific energy increases with decreasing depth of cut. This can be explained by the so-called size effect. The cross section of the chip, which is smaller for smaller depths of cut, possess different mechanical properties at microscale as compared with macroscale, due to the existence of fewer numbers of dislocations, grit faults and inclusions. Therefore, the micro hardness increases, resulting in an increase of the specific energy in grinding, see also Ref [2].

Table 1: Experimental measurements and calculated results

(a) Depth of cut, a=0.02 mm

	Experimental	Calculated				
Grinding wheel	P'_t (W/mm)	F'_t (N/mm)	u (J/mm^3)	ε (%)	l_c (mm)	Q (W/mm^2)
No. 1	143.5	5.13	53.81	0.885	2.24	56.77
No. 2	164.0	5.86	61.50	0.899	2.24	65.94
No. 3	176.0	6.29	66.00	0.906	2.24	71.30
No. 4	132.5	4.73	49.69	0.875	2.24	51.85
No. 5	170.5	6.09	63.94	0.903	2.24	68.84
No. 6	141.0	5.04	52.88	0.883	2.24	55.65

(b) Depth of cut, a=0.05 mm

	Experimental	Calculated				
Grinding wheel	P'_t (W/mm)	F'_t (N/mm)	u (J/mm^3)	ε (%)	l_c (mm)	Q (W/mm^2)
No. 1	277.5	9.95	41.78	0.851	3.54	67.06
No. 2	288.5	10.29	43.20	0.856	3.54	69.75
No. 3	298.5	10.66	44.78	0.861	3.54	72.72
No. 4	256.0	9.14	38.40	0.838	3.54	60.70
No. 5	277.5	9.91	41.63	0.851	3.54	66.78
No. 6	378.5	13.52	56.78	0.891	3.54	95.35

4. Results and discussion

4.1 Temperature fields

The parameters reported on the previous paragraph are applied to the model. In Fig 3 (a) and (b) variations of the temperatures on the surface of the workpiece, for different grinding wheels and with distance x from the left edge of the workpiece are presented, for each depth of cut. The temperature fields appear to be the same for the same depth of cut and the only difference is the maximum temperature reached for each grinding wheel. From the same figures it is revealed that the temperatures are higher in the regions on the back of the wheel, therefore, it seems that, it is more critical to direct the coolant to this side, in order to prevent the damage of the surface integrity due to the temperature rise.

From the same figures it can be concluded that wheel No. 4 has the lower maximum temperature for both depth of cut, whilst when grinding with wheel No. 6 a significant deviation in temperature between the two cases. This irregularity may be attributed either to the wheel specification being not suitable for the cutting conditions and so the grains are overloaded, or to the increase of the specific energy due to friction. The latter can be explained by the bigger radius in the workpiece-wheel contact zone, when the depth of cut is bigger, leading to the increase of the adhesive effect between the workpiece material and the wheel. The particles that are adhered to the wheel increase the friction surfaces, leading to the consumption of more energy. Such a phenomenon is not rare in grinding technology; it can be avoided by using the right wheel or coolant.

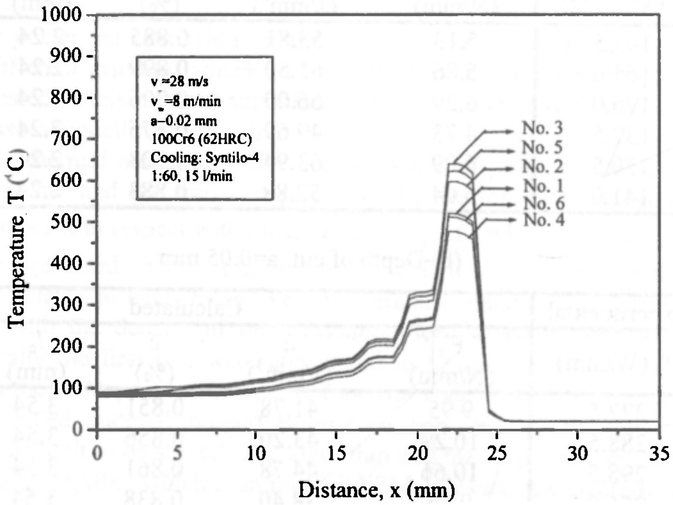

Fig.3 (a): Temperature variation on the surface of the workpiece for depth of cut 0.02 mm

The individual results obtained for grinding wheel No.3, can be seen in Fig 4 (a) and (b) for depth of cut 0.02 mm and 0.05 mm, respectively; the maximum temperature and the temperature fields for a specific step of the analysis are illustrated, in both isothermal bands within all the workpiece and isothermal lines in the region underneath the grinding wheel, where the maximum temperature appears.

In Fig 5 (a) and (b) the temperatures on the surface (y=0) and underneath it (y>0), for grinding wheel No. 4 are presented. In these diagrams y (mm) is the distance of the nodes of the mesh of the finite element model from the surface, C is the center of the heat source and the region $0\text{-}l_{ci}$ is the current position of the heat source, where l_{ci}, i=1,2, is the geometrical contact length between the grinding wheel and the workpiece.

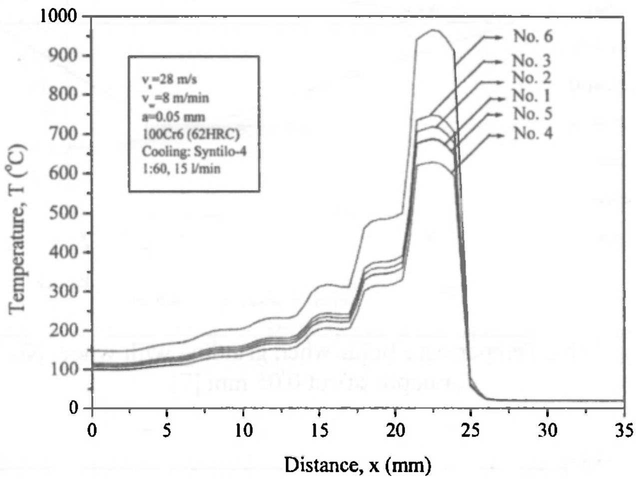

Fig. 3 (b): Temperature variation on the surface of the workpiece for depth of cut 0.05 mm

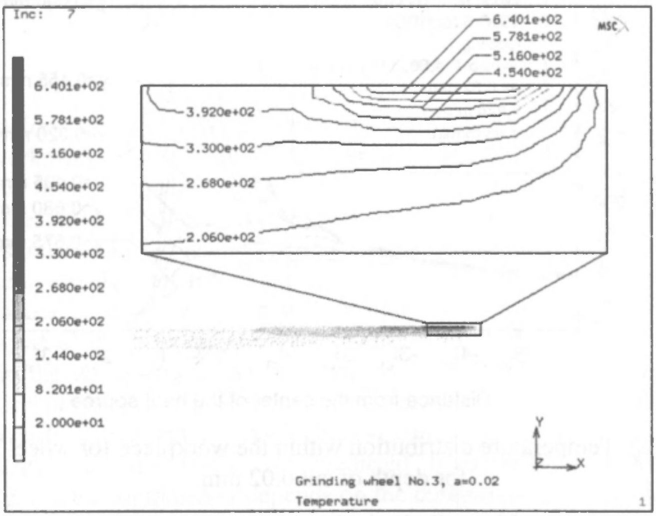

Fig. 4 (a): Temperature fields when grinding with wheel No.3, for depth of cut0.02 mm [7]

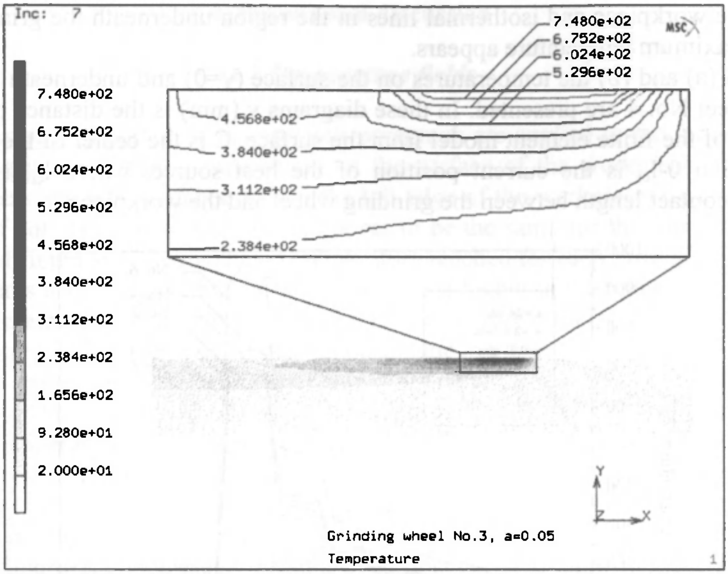

Fig. 4 (b): Temperature fields when grinding with wheel No.3, for depth of cut 0.05 mm [7]

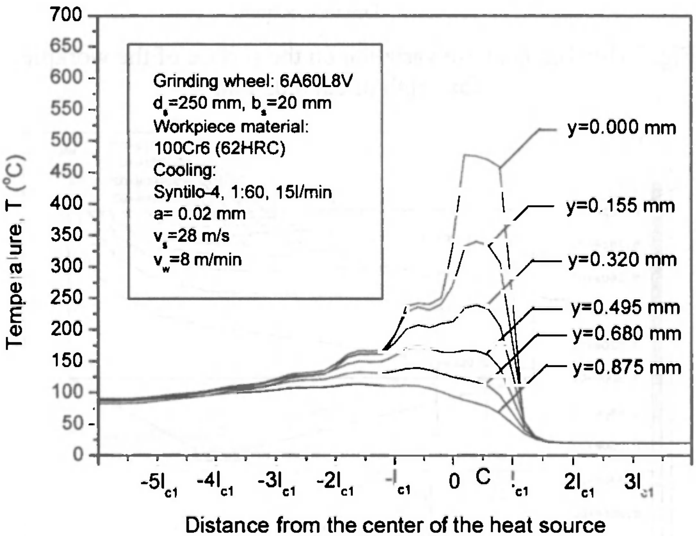

Fig.5 (a): Temperature distribution within the workpiece for wheel No.4, for depth of cut 0.02 mm

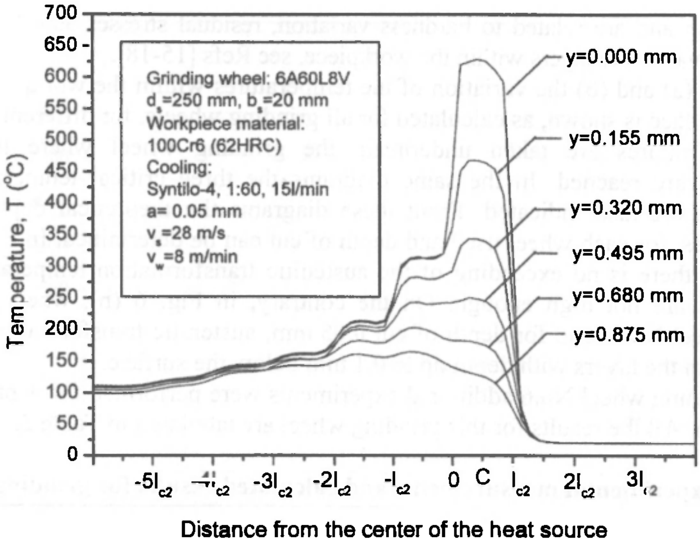

Fig. 5 (b): Temperature distribution within the workpiece for wheel No.4, for depth of cut 0.05 mm

From these figures it can be concluded that the maximum temperature appears to be reported very close to the center of the heat source and that the temperatures below the surface and especially for y>0.320 mm are approximately half than those on the surface of the workpiece. Furthermore, the regions in front of the heat source that are more than 1 l_{ci} away from the center of the heat source are not yet affected, while the regions even at a distance of 5.5 l_{ci} from the same point are still thermally loaded.

4.2 Heat affected zones

As noted before, the high temperatures that usually appear in grinding have a negative effect on the workpiece. The surface of the workpiece and also the layers that are near the surface and have been affected by the heat loading during the grinding process consist the heat affected zones of the workpiece. The excessive temperature in these zones contributes to residual stresses, microcracking and tempering and may cause microstructure changes, which result to hardness variations of the workpiece surface. Steels that cool down quickly from temperatures above the austenitic transformation temperature undergo metallurgical transformations; as a result, untempered martensite is produced which forms the so-called "white layer" in the workpiece. Excessive heat may also lead to metallurgical bum of the workpiece, which produces a bluish color on the surface of the processed material due to oxidation. If the critical temperatures at which these transformations take place are known, the size of the heat affected zones can be also "predicted" from the FEM model. The actual size of these zones and their composition depends on the duration of thermal loading, except the maximum temperature reached. The three critical temperatures for the 100Cr6 steel are [2]: T_T=150 °C for tempering, T_M=250 °C for martensitic and, T_A=800 °C for austenitic transformation and are related to hardness variation, residual stresses and the formation of untempered martensite layers within the workpiece, see Refs [15-18].

In Fig 6 (a) and (b) the variation of the temperatures within the workpiece with depth below the surface is shown, as calculated for all grinding wheels, for different depths of cut. These temperatures are taken underneath the grinding wheel where the maximum temperatures are reached. In the same diagrams the three critical temperatures for the 100Cr6 steel are also indicated. From these diagrams the theoretical depth of the heat affected zones, for each wheel used and depth of cut can be determined. In Fig. 6 (a) it can be seen that there is no exceeding of the austenitic transformation temperature since the temperatures are not high enough. On the contrary, in Fig. 6 (b), when grinding with grinding wheel No. 6 and for depth of cut 0.05 mm, austenitic transformation temperature is exceeded in the layers with depth up to 0.1 mm below the surface.

For grinding wheel No.6 additional experiments were performed for depths of cut 0.01 and 0.03 mm. All the results for this grinding wheel are tabulated in Table 2.

Table 2: Experimental measurements and calculated results for grinding wheel No.6

	Experimental	Calculated				
Depth of cut (mm)	P'_t (W/mm)	F'_t (N/mm)	u (J/mm^3)	ε (%)	l_c (mm)	Q (W/mm^2)
0.01	102.8	3.66	76.88	0.919	1.58	59.59
0.02	141.0	5.04	52.88	0.883	2.24	55.65
0.03	202.5	7.23	50.63	0.877	2.74	64.87
0.05	378.5	13.52	56.78	0.891	3.54	95.35

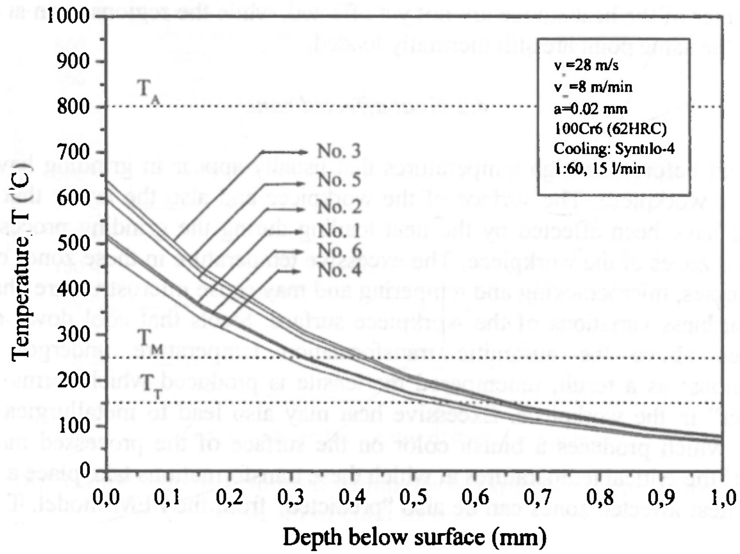

Fig. 6 (a): Variation of temperature with depth below surface when grinding 100Cr6 steel with various grinding wheels for a depth of cut 0.02 mm

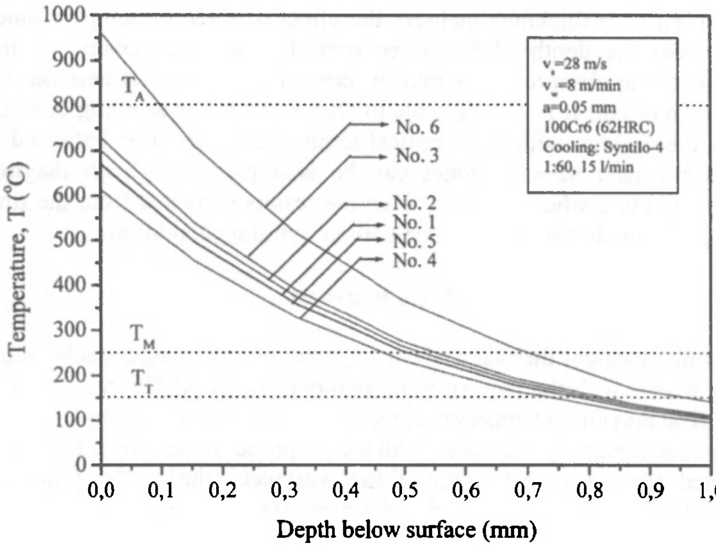

Fig. 6 (b): Variation of temperature with depth below surface when grinding 100Cr6 steel with various grinding wheels for a depth of cut 0.05 mm

By using these data a diagram is presented, see Fig. 7, to approximately predict the temperatures on the surface and within the workpiece for different values of the equivalent chip thickness, h_{eq} (mm), which is calculated as

$$h_{eq} = \frac{v_w}{v_s} a \tag{7}$$

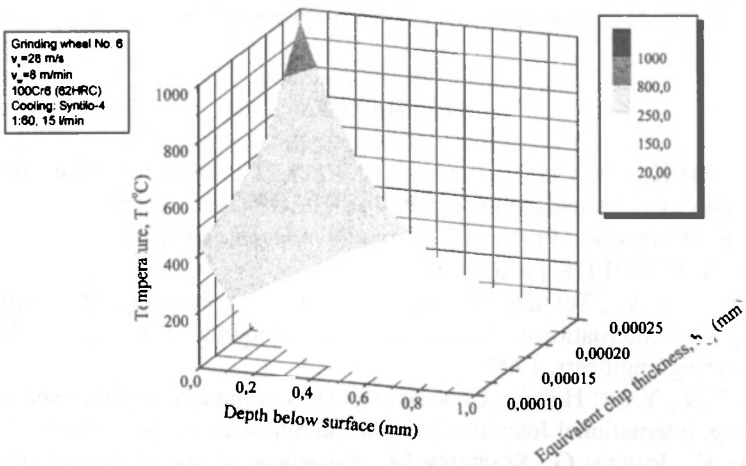

Fig. 7: Variation of temperature with depth below surface and equivalent chip thickness, h_{eq}, when grinding 100Cr6 steel with grinding wheel 6.

The equivalent chip thickness includes the effect of three grinding parameters and is more suitable than the depth of cut to be used for the optimization of the grinding parameters. In order to observe, or to limit, its critical value it is not necessarily needed to decrease the depth of cut; it is also possible to alter suitably the grinding conditions. In the same diagram the regions within the critical temperatures are also indicated by contour bands, so that the heat affected zones can be also predicted. Such diagrams can be constructed for the other wheels as well, from the results extracted from the finite element model and used as a guide for choosing the optimal grinding conditions.

5. Conclusions

From the finite element thermal analysis of grinding of hardened steels with aluminium oxide grinding wheels with the implicit finite element code MARC some useful conclusions may be drawn. The maximum temperature and the distribution of the temperature fields in the workpiece can be successfully calculated with the proposed model, when knowing the power or the tangential force per unit width of the workpiece during the process. From the temperature fields derived from the model, the heat affected zones of the workpiece can be predicted, considering the critical temperatures for tempering, martensitic and austenitic transformation. Furthermore, it is possible to correlate the temperature fields and thus the heat damage induced to the workpiece with kinematical and geometrical parameters of the process in order to find the optimal grinding conditions. Note that, the calculation of temperature is also based on kinematical and geometrical parameters. That allows for the monitoring of the process without using any temperature measurement devices.

The proposed model is relatively simple and very fast, since it takes only a few seconds for running on a modern PC; the total time depends on the number of steps and the parameters applied. It provides a very reliable tool and could replace difficult and time-consuming experiments. Furthermore, it can provide data, like the temperature fields in the workpiece, that it could be very laborious to obtain otherwise.

REFERENCES

1. TÖNSHOFF H.K. PETERS J., INASAKI I., PAUL T.: *Modelling and simulation of grinding processes*, Annals of the CIRP, Vol. 41/2/1992, pp. 677-688.
2. SNOEYS R., MARIS M., PETERS J.: *Thermally induced damage in grinding*, Annals of the CIRP, Vol.27/2/1978, pp. 571-581.
3. HOFFMEISTER H.W. WEBER T.: *Simulation of grinding by means of the finite element analysis*, 3rd International Machining and Grinding Conference, Society of Manufacturing Engineers, 1999.
4. MOULIK P.N., YANG H.T.Y., CHANDRASEKAR S.: *Simulation of thermal stresses due to grinding*, International Journal of Mechanical Sciences, 43, pp. 831-851, 2001.
5. WEINERT K., JOHLEN G., SCNEIDER M.: *Experimental and numerical studies of the grinding process on tool life*, Production engineering, Vol. V/2,1998, pp. 9-14.
6. MAHDI M., ZHANG L.: *The finite element thermal analysis of grinding processes by ADINA*, Computers and Structures Vol. 56, No. 2/3, pp. 313-320, 1995.

7. MAMALIS A.G., KUNDRÁK J., MANOLAKOS D.E. GYÁNI K., MARKOPOULOS A. HORVÁTH M.: *Effect of the workpiece material on the heat affected zones durin grinding: numerical simulation*, International Journal of Advanced Manufacturing Technology 4/10/2002 (In press)
8. MAMALIS A.G., KUNDRÁK J., MANOLAKOS D.E., MARKOPOULOS A., CHRISTOFOROU G.: *Numerical analysis of surface grinding: comparison between 2D and 3D modelling* Proc. of the microCAD 2003 International Computer Science Conference, Miskolc, Hungary, 2003 (In press).
9. JAEGER J.C.: *Moving sources of heat and the temperature at sliding contacts*, Journal and Proceedings of the Royal Society of New South Wales, Vol. 76/3, pp. 263-264, 1942.
10. OUTWATER J.O., SHAW M.C.: *Surface temperatures in grinding*, Transactions of ASME, 74, pp. 73-86, 1952.
11. DES RUISSEAUX N.R., ZERKLE R.D.: *Temperature in semi-infinite and cylindrical bodies subjected to moving heat sources and surface cooling*, Journal of Heat Transfer, 92, pp. 456-464, 1970.
12. GUO C., MALKIN S., *Energy partition and cooling during grinding*, 3rd International Machining and Grinding Conference, Society of Manufacturing Engineers, 1999.
13. ROWE W.B., MORGAN M.N., ALLANSON D.A.: *An advance in the modelling of thermal effects in the grinding process*, Annals of the CIRP, Vol.40/1/1991, pp. 339-342.
14. MALKIN S.: *Burning limit for surface and cylindrical grinding of steels*, Annals of the CIRP, Vol. 27/1/1978, pp. 233-236.
15. SHAW M.C., VYAS A.: *Heat affected zones in grinding steel*, Annals of the CIRP, Vol.43/1/1994, pp. 279-282.
16. ZHANG L., MAHDI M.: *Applied mechanics in grinding – IV. the mechanism of grinding induced phase transformation*, International Journal of Machine Tools and Manufacture, Vol. 35, No. 10, pp. 1397-1409, 1995.
17. CHANG C.C., SZERI A.Z.: *A thermal analysis of grinding*, Wear, 216, pp. 77-86, 1998.
18. ROWE W.B., PETIT J.A., BOYLE A., MORUZZI J.L.: *Avoidance of thermal damage in grinding and prediction of the damage threshold*, Annals of the CIRP, Vol.37/1/1988, pp. 327-330.

Appendix 1

In this appendix a concise description of the mathematical formulation used for heat transfer analysis by MARC is given. The formulae and the algorithm used are taken by the training guide of MARC Mentat, supplied with the program.

The heat transfer problem can be written, as known, as a differential equation

$$[C]\{\dot{T}\}+[K]\{T\}=\{Q\} \tag{8}$$

where $[C]$ is the heat capacity matrix, $[K]$ the conductivity and convection matrix, $\{T\}$ the vector of the nodal temperatures and $\{Q\}$ the vector of nodal fluxes. In the case of a steady state problem, where $\dot{T}=\frac{\partial T}{\partial t}=0$, the solution can be easily obtained by a matrix inversion

$$\{T\}=[K]^{-1}\{Q\} \tag{9}$$

In the case of transient analysis, where $\dot{T}\neq 0$, which is the case described in this paper, the nodal temperature is approximated at discrete points in time as

$$\{T\}^n=\{T\}(t_0+n\Delta t) \tag{10}$$

MARC program is using a backward difference scheme to approximate the time derivative of the temperature

$$\{\dot{T}\}^n \cong \frac{\{T\}^n-\{T\}^{n-1}}{\Delta t} \tag{11}$$

which, when substituted in equation (8), results in the finite difference scheme

$$\left(\frac{[C]}{\Delta t}+[K]\right)\{T\}^n-\frac{[C]}{\Delta t}\{T\}^{n-1}=\{Q\} \tag{12}$$

that gives the solution of the differential equation (8).